

## Three-dimensional effects of supersonic cavity flow due to the variation of cavity aspect and width ratios

Chel-hun Woo<sup>1</sup>, Jae-soo Kim<sup>2,\*</sup> and Kyung-hwan Lee<sup>3</sup>

<sup>1</sup>Flight Dynamics Section, KHP Program Division, Korea Aerospace Industries, 802 Yucheon-ri, Sanam-myeon, Sacheon, 664-710, Korea

<sup>2</sup>Department of Aerospace Engineering, Chosun University, 375 Seosuk-dong, Dong-gu, Gwangju, 501-759, Korea

<sup>3</sup>Department of Aerospace Engineering, Sunchon National University, 315 Maegok-dong Suncheon, 540-742, Korea

(Manuscript Received April 11, 2007; Revised November 8, 2007; Accepted November 9, 2007)

---

### Abstract

Unlike the steady closed-type supersonic cavity flow, open-type cavity flow is divided into internal and external flows by turbulent shear layer. The cavity flow may cause resonance phenomena due to pressure oscillation, depending on the cavity geometry and the flow conditions. These phenomena may induce noise generation, structural damage, and aerodynamic instability. In this research, the flow characteristics of three-dimensional supersonic cavity flow of Mach number 1.5 were analyzed with the variations of aspect ratio and width ratio. Three-dimensional unsteady compressible Reynolds-averaged Navier-Stokes (RANS) equations were used with a turbulence model. For numerical calculations, the 4th-order Runge-Kutta method and the FVS method with van Leer's flux limiter were applied. The numerical calculations were performed by using a parallel processing program with 16 CPUs. The sound pressure level (SPL) spectra of pressure variations were analyzed at the point of cavity leading edge. The correlation of pressure distribution (CPD) was also analyzed for the propagation of dominant oscillation pressure waves with respect to the reference point of the cavity leading edge. The dominant oscillation frequency was compared with the oscillation modes of Rossiter's formula. Oscillation Mode 2 appeared as a dominant oscillation frequency regardless of the aspect ratio of cavity in the two-dimensional flow. Oscillation Modes 1 and 2 appeared in three-dimensional cavities of small aspect ratios. However, as the aspect or the width ratio increases, only the mode 2 or 3 frequency appeared as a dominant oscillation frequency.

*Keywords* : Three-dimensional cavity flow; Unsteady compressible flow;  $\kappa - \omega$  Turbulence model; SPL (Sound Pressure Level); CPD (Correlation of Pressure Distribution)

---

### 1. Introduction

The characteristics of the pressure oscillation over a cavity are determined by the flow conditions and the cavity geometry. Generation and strength of the pressure oscillation are known to be determined by a balance between the energy supplied by free-stream flow and various energy dissipations such as viscosity dissipation, acoustic dissipation, and mass exchange

caused by convection. Since this pressure oscillation can induce noise generation, structural damages, and adverse effects on aerodynamic performance and stability, many researches have been made since the 1950s. The cavity flows are classified into open-type ( $L/D < 10$ ) and closed-type ( $L/D > 13$ ) according to the aspect ratio of the cavity. In the closed-type cavity, the shear layer generated at the leading edge collides with the cavity floor. The layer is reflected from the floor, expansion waves are formed, and the flow escapes from the trailing edge. Therefore, two small separated zones are formed in the cavity. The reso-

---

\*Corresponding author. Tel.: +82 62 230 7080, Fax.: +82 62 230 7139  
E-mail address: jsckim@mail.chosun.ac.kr  
DOI 10.1007/s12206-007-1103-9

nance condition is not severe because the flow is stable. In the open-type cavity, on the other hand, the free-stream shear layer generated at the leading edge is reattached to the trailing edge and divides the flow into internal and external flows in an unstable manner. The interaction between the internal and the external flows causes pressure change, resulting in a severe oscillation condition [1, 2].

Initial researches for oscillation prediction models were carried out, using empirical methods, by Krishnamurthy [3], Rossiter [4] and Heller et al. [5], which are still widely used. The numerical analysis for the two-dimensional flow and the analysis of turbulence flow characteristics were started by Rowley et al. [6], Sinha et al. [7], and others. Gharib & Roshko [8] demonstrated through numeric analysis that the shear layer mode changed to the wake mode as the aspect ratio (the length to depth ratio,  $L/D$ ) was increased for two-dimensional cavity flow. Chingwei & Philip [9] showed through numerical analysis that the shear layer mode rather than the wake mode was dominant in the three-dimensional flow. Woo, Kim and Lee [10] studied the flow over tandem cavities for the two-dimensional and the three-dimensional flows. However, they were only able to show fragmentary numerical analysis results due to the limited massive computation capability.

According to the researches by Rossiter [4] and Heller et al. [5], the dominant oscillation frequency in cavity flow is determined as mode 1, 2, 3, or others depending on the cavity geometry and the flow conditions. Rossiter's formula [4] was developed to predict the resonance frequency based on the circulation structure of fluctuation, which represents the non-dimensional oscillation number (Strouhal Number) for the circulation process between the vortex that flows in the shear layer and the pressure wave that is reflected from the trailing edge as mode 1, 2, 3, .... This formula has the advantage of easily predicting the dominant oscillation frequency just with Mach number and the cavity aspect ratio. It has been widely used even today.

In this research, the effect of various aspect ratios ( $L/D$ s) and width ratios ( $W/D$ s) of the cavity on three-dimensional supersonic cavity flow was analyzed. The three-dimensional unsteady compressible Reynolds-averaged Navier-Stokes (RANS) equations were adopted with a  $k-w$  turbulence model. A 4th order Runge-Kutta method and an FVS (flux vector split) technique with van Leer's flux limiters were

used. Numerical analysis was done by using MPI parallel processing techniques with 16 CPUs. The numerical analysis results were verified by a comparison between the non-dimensional oscillation frequency with Rossiter's formula [4] and the empirical results of Zhang & Edwards [11].

In order to analyze the three-dimensional flow characteristics, the numerical analyses were performed for various width ratios from 1 to 5 with the aspect ratios of 2, 3 and 4, which have open-type cavity flow characteristics. According to the analysis, the dominant oscillation frequency corresponding to Oscillation Mode 2 appeared regardless of the aspect ratio in the two-dimensional flow. On the other hand, the dominant oscillation frequencies corresponding to Oscillation Modes 1 and 2 appeared for the aspect ratio of 2 regardless of the width ratio in the three-dimensional flow. For the aspect ratio of 3, Oscillation Modes 1 and 2 appeared when the width ratio was lower, and only Oscillation Mode 2 appeared when the width ratio was increased. As the aspect ratio was increased to 4, Oscillation Modes 1 and 2 were weakened considerably and Oscillation Mode 3 appeared to be dominant. These results indicate that the mode change is an important characteristic in the three-dimensional flow, although the dominant frequency is almost fixed as mode 2 in the two-dimensional flow.

## 2. Governing equations and numerical analysis

The three-dimensional unsteady compressible Reynolds-averaged Navier-Stokes equation is non-dimensionalized, as follows.

$$\frac{\partial \bar{Q}}{\partial t} + \frac{\partial \bar{E}}{\partial \xi} + \frac{\partial \bar{F}}{\partial \eta} + \frac{\partial \bar{G}}{\partial \zeta} = \frac{\partial \bar{E}_v}{\partial \xi} + \frac{\partial \bar{F}_v}{\partial \eta} + \frac{\partial \bar{G}_v}{\partial \zeta} + \bar{S} \quad (1)$$

Cavity depth ( $D$ ), free-stream velocity and density are the non-dimensional characteristic values, and  $t$ ,  $\xi$ ,  $\eta$  and  $\zeta$  indicate non-dimensional time and generalized coordinates.  $\bar{E}$ ,  $\bar{F}$ ,  $\bar{G}$  and  $\bar{E}_v$ ,  $\bar{F}_v$ ,  $\bar{G}_v$  are the generalized coordinate flux vectors expressed as functions of the transform matrix [12].  $\bar{S}$  is the source term in the turbulence model, when the turbulence model equations are written in the form of flux vector like the Navier-Stokes equation. Wilcox's  $k-\omega$  turbulence model is used [13, 14]. The model was originally developed for incom-

pressible flow and modified for compressible flow. Bardina et al. [15] showed in their paper on the turbulence modeling test that the result of Wilcox's model was reasonable in compressible flow. An explicit 4th-order Runge-Kutta method was applied for time discretization and a 2nd order flux vector split (FVS) method with van Leer's flux limiters was used for spatial discretization. The In-House code including message passing interface (MPI) parallel processing technique was used for calculations.

The cavity geometry and the flow conditions are based on the experimental models of Zhang & Edwards [11]. The cavity depth ( $D$ ) of 15mm and the cavity aspect ratios ( $L/D$ ) of 2, 3, and 4 were adopted. Calculation was performed for the flow with Reynolds number of  $4.5 \times 10^5$  and Mach number 1.5 for both two-dimensional and three-dimensional analyses. For the three dimensional analysis, numerical calculation was carried out for the width ratio of 1.0 through 6.0.

Fig. 1 shows a part of a three-dimensional grid system with aspect ratio of 3 and width ratio of 4. The grids are concentrated near the wall surface. The dimensionless sub-layer scaled distance  $y^+$  ( $= y\sqrt{\rho_w\tau_w/\mu_w}$ ) of the first grid point is about 0.01~1.5. According to the research by Abdol-Hamid et al. [16], reasonable results can be seen when  $y^+$  of the first grid point is less than 10 even in a large separated flow. Therefore, the turbulence flow was directly calculated without wall function. The far boundary condition was set at 7 times the distance of depth ( $D$ ). Several sets of grids were tested for grid convergence. Finally, a grid system of  $351 \times 100$  for the upper zone and  $100 \times 70$  for the cavity was chosen for the two-dimensional case, and it was varied from  $140 \times 40 \times 40$  to  $140 \times 40 \times 90$  for the upper zone and from  $50 \times 30 \times 20$  to  $50 \times 30 \times 70$  for the cavities of three-dimensional

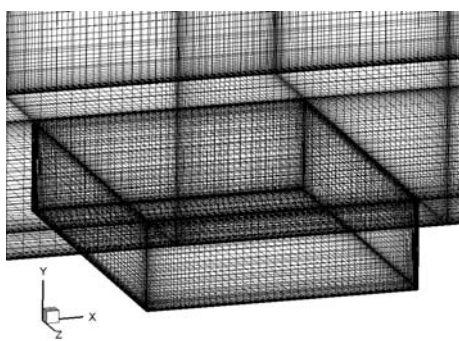


Fig. 1. Computational grids for three-dimensional cavity.

cases.

### 3. Results and discussion

For the analysis of flow characteristics, the dominant oscillation frequency was calculated from the spectra of sound pressure level (SPL) at the cavity leading edge center point. The correlation of pressure distribution (CPD) also analyzed to observe the transmission process of dominant oscillation frequency with respect to the reference point of cavity leading edge.

Fast Fourier transform (FFT) was applied to analyze the spectra of sound pressure level and the correlation of pressure distribution, which are expressed in the following equations.

$$SPL(f) = 20 \log_{10}(FFT(p)/p_{ref})(dB) \quad (2)$$

$$Re(CPD(f)) = 10 \log_{10}(Re((FFT_{ref}(p)/p_{ref}) \cdot (FFT(p)/p_{ref}))) (dB) \quad (3)$$

$$p_{ref} = 2 \times 10^{-5} (N/m^2)$$

where  $f$ ,  $p$ , and  $p_{ref}$  are frequency, pressure, and reference sound pressure, respectively.  $SPL(f)$  and  $Re(CPD(f))$  represent the spectra of sound pressure level and the real value of correlation of pressure distribution with the reference point of leading edge center, respectively [17].  $SPL(f)$  and  $Re(CPD(f))$  represent the dominant frequencies and the characteristics of propagation of dominant pressure oscillation, respectively.

Fig. 2 shows a comparison between the non-dimensional Strouhal numbers [4] obtained by  $St = fL/U = (n - \gamma)/(1/k_v - M)$  and the experimental value of Heller et al. [5] and the results of this research.  $n$  is the number of oscillation mode,  $k_v$  ( $=0.57$ ) is the constant representing the vortex convection speed as a fraction of the free-stream flow speed at the cavity entrance,  $M$  is the free-stream Mach number, and  $\gamma$  ( $=0.25$ ) is a constant obtained from the experiments. The 2nd mode Strouhal number of two-dimensional and three-dimensional flows is 0.57, which is almost the same as Rossiter's formula [4] and the experimental value of Heller et al. [5]. In the three-dimensional flow, the 1st mode Strouhal number is observed as 0.269, which is similar to the value of the 1st mode of Rossiter's formula [4].

Table 1. Comparison of dominant frequency (mode number  $n=2$ ).

	Zhang & Edward [11]	Rossiter's Eq [4]	Two-dimensional flow	Three-dimensional flow
$L/D = 3$	5.90kHz	5.45kHz	5.40kHz	5.40kHz

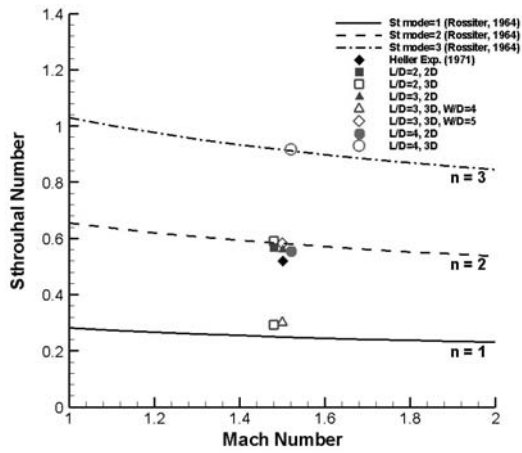


Fig. 2. Non-dimensional resonant frequencies as a function of Mach number.

Table 1 shows the comparison between the frequency characteristics of this study and those obtained by Rossiter [4] and Zhang and Edwards [11], in which the present results appear to be very reasonable.

**3.1 Cavity flow for the aspect ratio (L/D) of 2**

The variations of dominant oscillation frequency were analyzed, with the aspect ratio of 2 and the width ratio changing from 1 to 4. Figs. 3 and 4 show the pressure histories at the points of cavity leading edge and its bottom center. The amplitude of pressure change of the two-dimensional cavity was larger than that of the three-dimensional cavity. The pressure histories of the three-dimensional cavities were almost similar to each other regardless of their width ratio. The period of the three-dimensional flow was about twice as much as that of the two-dimensional flow. It is because the three-dimensional flow had two dominant frequencies of modes 1 and 2, while the two-dimensional flow had one dominant frequency of mode 2. The frequency of mode 1 was about half the frequency of mode 2. Compared to the two-dimensional cavity, the three-dimensional cavity had lower pressure amplitude due to the flows from the z-transverse direction.

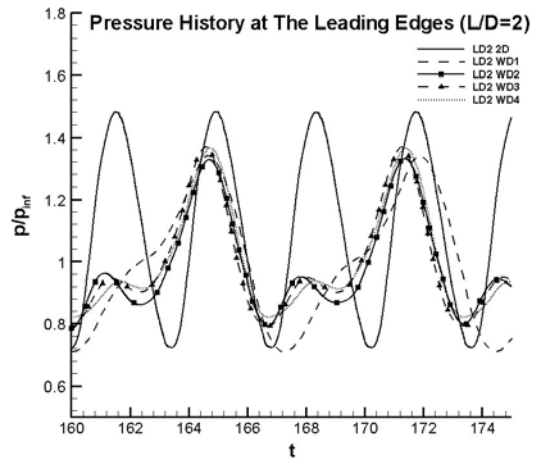


Fig. 3. Pressure history of the leading edge ( $z/D=50\%$ ).

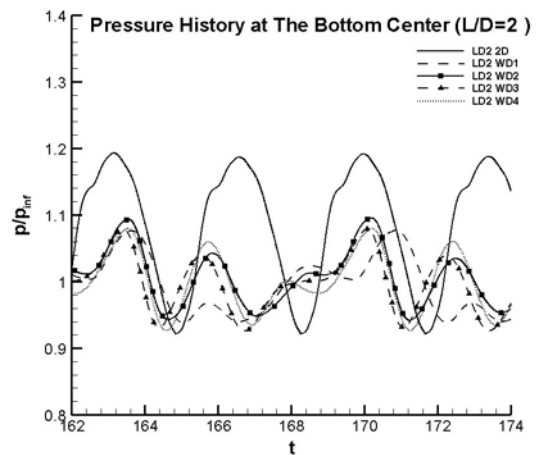


Fig. 4. Pressure history of the bottom center ( $z/D=50\%$ ).

Fig. 5 shows the results of SPL of the dominant oscillation frequency observed for the two-dimensional and the three-dimensional cavities with width ratios of 2, 4 and 5. The peak of dominant oscillation frequency of the two-dimensional cavity was located in the 8.27 kHz band. This corresponds to Oscillation Mode 2 of Rossiter's formula [4]. Unlike the two-dimensional cavity, the three-dimensional cavity had the peaks at 4.24 kHz and 8.30 kHz bands regardless of the width ratio. These results agree, respectively, with Oscillation Modes 1 and 2 of Rossiter's formula [4], which imply that the dominant oscillation frequencies corresponding to Oscillation Modes 1 and 2 appear regardless of the width ratio in the three-dimensional flow.

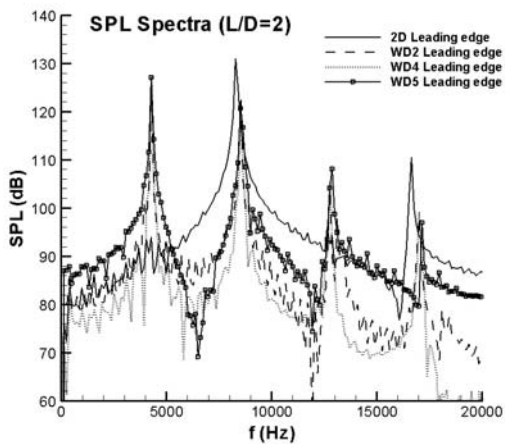


Fig. 5. SPL spectra at the leading edge.

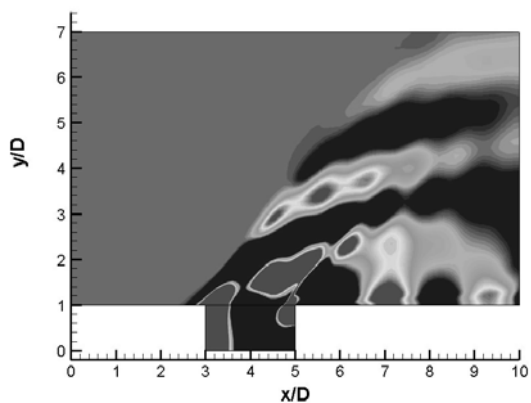


Fig. 8. Re(CPD) distribution of 2D cavity for the 8.27 kHz (Mode=2) band.

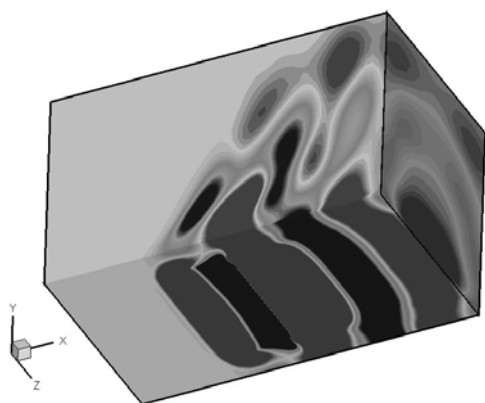


Fig. 6. Re(CPD) distribution of 3D cavity for the 4.24 kHz (Mode=1) band.

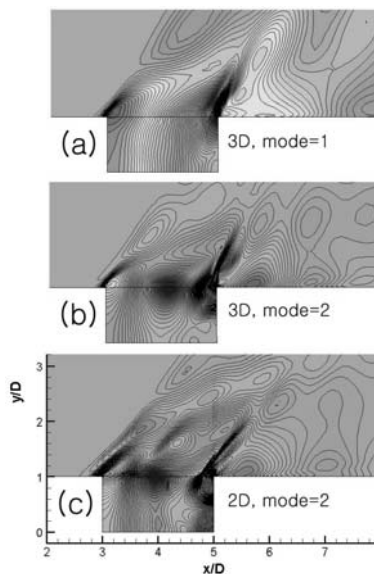


Fig. 9. Re(CPD) Contour lines for the dominant frequency.

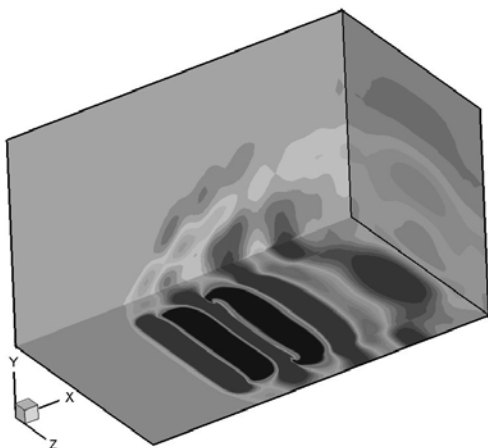


Fig. 7. Re(CPD) distribution of 3D cavity for the 8.27 kHz (Mode=2) band.

Figs. 6, 7 and 8 show the real part of the correlation of pressure distribution (CPD) for the dominant pressure oscillation with respect to the reference point of the leading edge center. Figs. 6 and 7 show the CPD results of dominant oscillation frequencies of 4.24 kHz and 8.27 kHz for the three-dimensional cavity with the width ratio of 4. The CPD result of dominant oscillation frequency of 8.27 kHz for the two-dimensional cavity is shown in Fig. 8. Figs. 7 and 8 represent similar fluctuation transmission characteristics of Oscillation Mode 2 for the two-dimensional and the three-dimensional flows, respectively, while Fig. 6 shows that of mode 1 for the three-dimensional flow.

Fig. 9 shows the contour lines of the real part of CPD of the dominant oscillation frequency for the center section ( $z/D = 50\%$ ) of the three-dimensional and the two-dimensional cavity flows. Fig. 9 (a) shows that the contour lines of 4.24 kHz band correspond to Oscillation Mode 1 for the three-dimensional cavity flow. Figs. 9 (b) and 9 (c) show that the contour lines of 8.27 kHz band correspond to Oscillation Mode 2 for both the two-dimensional and the three-dimensional cavities.

**3.2 Cavity flow for the aspect ratio (L/D) of 3**

Figs. 10 and 11 show the pressure histories at the points of cavity leading edge and its bottom center when the aspect ratio was 3 and the width ratios were 1, 4, 5, and 6. The amplitude of pressure change of the two-dimensional cavity was larger than that of the

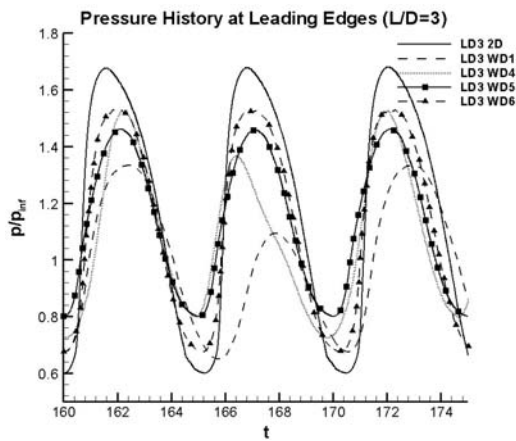


Fig. 10. Pressure history of the leading edge ( $z/D=50\%$ ).

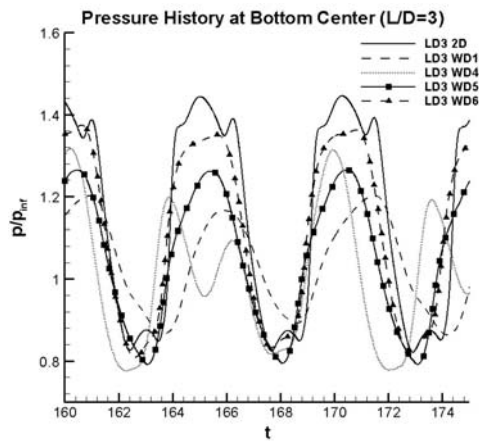


Fig. 11. Pressure history of the bottom center ( $z/D=50\%$ ).

three-dimensional cavity. The figures show that the period of pressure oscillation of the three-dimensional cavities with the width ratio of 5 and 6 is similar to that of the two-dimensional cavity.

Fig. 12 shows the results of SPL of the dominant oscillation frequencies observed for the two-dimensional and the three-dimensional cavities at the point of leading edge center. As the solid line representing the two-dimensional cavity was observed, it was shown that the dominant oscillation frequency was located in the 5.4 kHz band for the cavity with the aspect ratio of 3. This agrees with Oscillation Mode 2 of Rossiter's formula [4] and the experimental value of Zhang & Edwards [11]. For the three-dimensional cavities with the width ratios of 1 and 4, Oscillation Modes 1 and 2 of Rossiter's formula [4] were observed, which were located in the 2.9 kHz and 5.4 kHz bands, respectively. For the cavities with the aspect ratios of 5 and 6, however, the mode 1 frequency disappeared and only the mode 2 frequency appeared. These results confirm that the frequencies of modes 1 and 2 appear for the cavities with low width ratios and only the frequency of mode 2 appears for the cavities with the width ratio greater than 5, which appears the same for the two-dimensional cavities.

Figs. 13, 14 and 15 show the real part of CPD of the dominant oscillation frequencies. Figs. 13 and 14 show the CPD results for the dominant oscillation frequencies of 2.9 kHz and 5.4 kHz, respectively, for the three-dimensional cavity with the width ratio of 1. The CPD results of the dominant oscillation frequency of 5.4kHz are shown in Fig. 15 for the two-dimensional cavity. The transmission of pressure

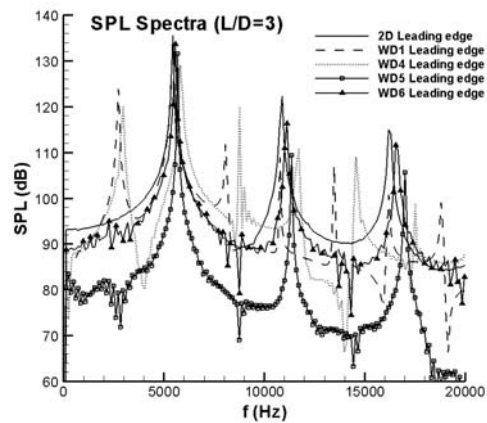


Fig. 12. SPL spectra at the leading edge ( $\Delta f = 118\text{Hz}$ ).

wave of the two-dimensional cavity was similar to the characteristics of Oscillation Mode 2 of the three-dimensional flow.

Fig. 16 shows the contour lines of real part of CPD of dominant oscillation frequency for the center section ( $z/D = 50\%$ ) of cavities. In Fig. 16 (a), the con-

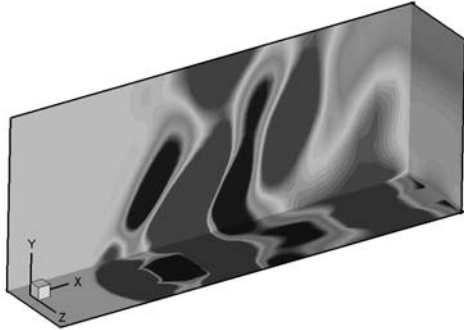


Fig. 13. Re(CPD) distribution of 3D cavity for the 2.9 kHz (Mode=1) band.

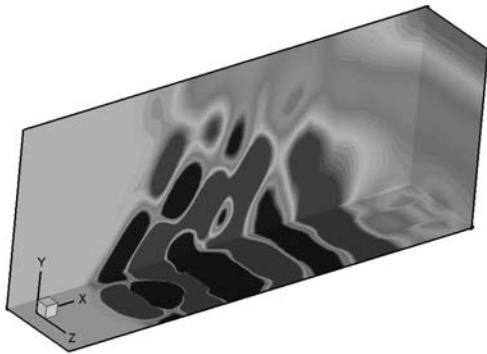


Fig. 14. Re(CPD) distribution of 3D cavity for the 5.4 kHz (Mode=2) band.

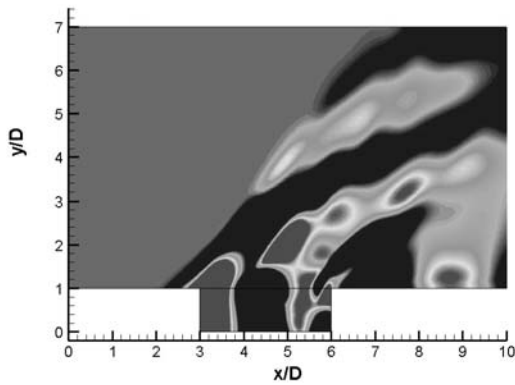


Fig. 15. Re(CPD) distribution of 2D cavity for the 5.4 kHz (Mode=2) band.

tour lines of the 2.9kHz band appear to be corresponding to Oscillation Mode 1. Fig. 16 (b) and 16 (c) show that the contour lines of the 5.4 kHz band correspond to Oscillation Mode 2 for both the two-dimensional and the three-dimensional cavities.

**3.3 Cavity flow for the aspect ratio (L/D) of 4**

Fig. 17 shows the results of SPL of the dominant frequencies observed for the two-dimensional cavity and the three-dimensional cavities with the width ratios of 2, 4 and 5. For the two-dimensional cavity, the dominant oscillation frequency was located in the

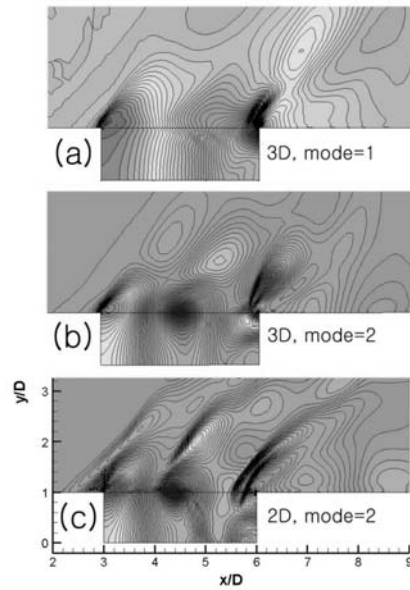


Fig. 16. Re(CPD) contour lines for the dominant frequency.

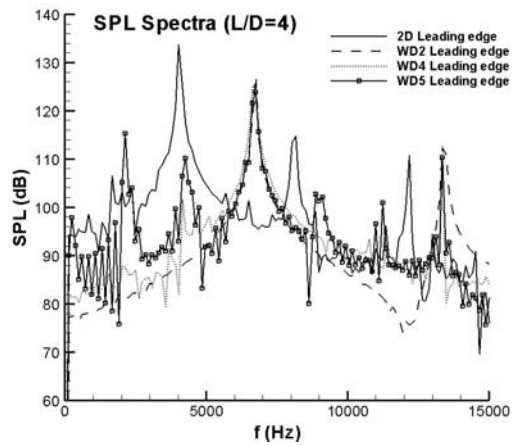


Fig. 17. SPL spectra at the leading edge.

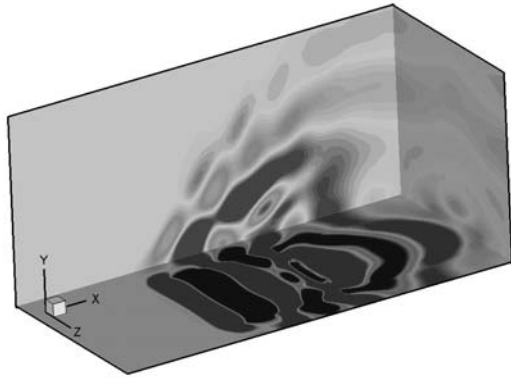


Fig. 18. Re(CPD) distribution of 3D cavity for the 6.62kHz (Mode=3) band.

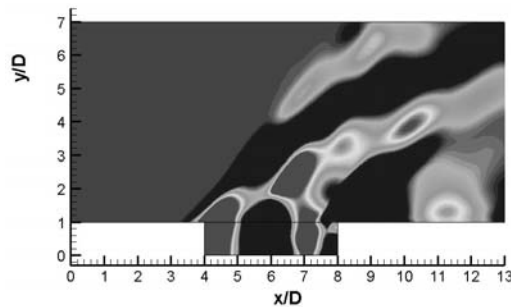


Fig. 19. Re(CPD) distribution of 2D cavity for the 4.03kHz (Mode=2) band.

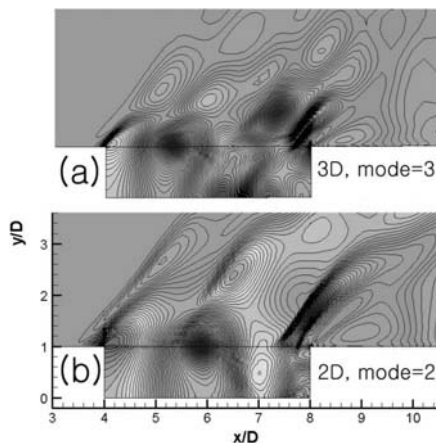


Fig. 20. Re(CPD) contour lines for the dominant frequency.

4.03 kHz (mode 2) band. The three-dimensional cavities had the peak in the 6.62 kHz (mode 3) band regardless of the width ratio. The results show that the

dominant frequency of the three-dimensional cavity was higher than that of the two-dimensional cavity, which corresponds to Oscillation Mode 3 of Rossiter's formula [4].

Fig. 18 shows the real part of CPD of the dominant frequency band of 6.62 kHz for the three-dimensional cavity with the width ratio of 4. Fig. 19 shows the CPD results of the dominant frequency of 4.03 kHz for the two-dimensional cavity. These Figs. show the transmission of pressure waves. Fig. 20 shows the contour lines of the real part of CPD of the dominant frequency of the two-dimensional cavity and the center section ( $z/D = 50\%$ ) of the three-dimensional cavities. Fig. 20 (a) shows the contour lines of 6.62 kHz band corresponding to Oscillation Mode 3 for the three-dimensional flow. Fig. 20 (b) shows the contour lines of 4.03 kHz band corresponding to Oscillation Mode 2 for the two-dimensional flow.

#### 4. Conclusions

The three-dimensional supersonic cavity flow characteristics were analyzed for the conditions of Mach number 1.5, with the aspect ratios ( $L/D$ ) of 2 ~ 4, the width ratios ( $W/D$ ) of 1 ~ 6, and Reynolds number ( $4.5 \times 10^5$ ), by using the unsteady Reynolds-averaged Navier-Stokes (RANS) equation with  $\kappa - \omega$  turbulence model. To analyze the cavity flow characteristic, the dominant frequency of pressure was examined at points on the leading edge. The dominant frequency was obtained by the SPL analysis for pressure changes. The CPD with the reference point of leading edge was analyzed to investigate how the pressure waves of dominant frequencies were transmitted to all regions of the flow. The dominant oscillation frequencies were then compared with the oscillation modes of Rossiter's formula (1964) and other experimental values. According to the analysis results, the dominant frequency corresponding to Oscillation Mode 2 appeared for the two-dimensional flow regardless of the aspect ratio. For the three-dimensional flow, on the other hand, the dominant frequencies changed with the aspect ratio and the width ratio. The dominant frequencies of modes 1 and 2 appeared regardless of the width ratio, when the aspect ratio was 2. The dominant frequencies changed from the combination of modes 1 and 2 to mode 2 as the width ratio was increased, when the aspect ratio was 3. When the aspect ratio was 4, only Oscillation Mode 3 appeared regardless of the width ratio. For the three-



dimensional flow, only the large mode frequencies appeared as the aspect ratio was increased, unlike the two-dimensional flow.

## References

- [1] X. Zhang and J. A. Edwards, Analysis of unsteady supersonic cavity flow employing an adaptive meshing refinement algorithm, *Computers & Fluids*, 25 (4) (1996) 373-393.
- [2] D. J. Maull and L. F. East, Three-dimensional flow in cavities, *J. Fluid Mechanics*, 16 (1963) 620-632.
- [3] K. Krishnamurty, Acoustic radiation from two-dimensional rectangular cutouts in aerodynamic surfaces, NACA TN-3487 (1955).
- [4] J. E. Rossiter, Wind-tunnel experiments on the flow over rectangular cavities at subsonic and transonic speeds, Aeronautical Research Council Reports and Memoranda 3438 (1964).
- [5] H. H. Heller, D. G. Holmes and E. E. Covert, Flow-induced pressure oscillations in shallow cavities, *Journal of Sound and Vibration*, 18 (1971) 545-553.
- [6] C. W. Rowley, T. Colonius and A. J. Basu, On self-sustained oscillations in two dimensional compressible flow over rectangular cavities, *J. Fluid Mech.*, 455 (2002) 315-346.
- [7] M. Sinha, B. J. York and S. M. Dash, Chidambaram, N., A Perspective on the Simulation of Cavity Aeroacoustics, *AIAA-98-0286* (1998).
- [8] M. Gharib and A. Roshko, The effect of flow oscillations on cavity drag, *J. Fluid Mechanics*, 177 (1987) 501-530.
- [9] M. S. Chingwei and J. M. Philip, Comparison of Two- and Three-Dimensional Turbulent Cavity Flows, *AIAA A01-16385* (2001).
- [10] Woo, Kim and Lee, Analysis of two dimensional and three dimensional supersonic turbulence flow around tandem cavities, *KSMIE Int. J.*, 20 (8) (2006) 1256-1265.
- [11] X. Zhang and J. A. Edwards, Experimental investigation of supersonic flow over two cavities in tandem, *AIAA J.* 30 (5) (1992) 1182-1190.
- [12] K. C. Hoffmann and S. T. Chiang, Computational Fluid Dynamics for Engineers, Engineering Education System USA, (1993).
- [13] D. C. Wilcox, Reassessment of the scale determining equation for advanced turbulence models, *AIAA J.* 19 (2) (1988) 248-251.
- [14] S. P. Pao and K. S. Abdol-Hamid, Numerical Simulation of Jet Aerodynamics Using the Three-Dimensional Navier-Stokes Code PAB3D, NASA TP 3596 (1996).
- [15] J. E. Bardina, P. G. Huang and T. J. Coakley, Turbulence Modeling Validation, Testing, and Development, NASA TM 110446 (1997).
- [16] C. S. Abdol-Hamid, B. Lakshmanan and J. R. Carlson, Application of Navier-Stokes Code PAB3D with Turbulence Model to Attached and Separated Flows, NASA TP 3480 (1975).
- [17] D. E. Newland, An Introduction to Random Vibrations, Spectral and Wavelet Analysis, Longman Press, Third edition (1993).